

Lawrence Berkeley National Laboratory

LBL Publications

Title

LEED INTENSITY ANALYSIS OF THE STRUCTURE OF COADSORBED BENZENE AND CO ON Rh(III)

Permalink

<https://escholarship.org/uc/item/1bb8r0pn>

Author

Lin, R.F.

Publication Date

1986-05-01



Lawrence Berkeley Laboratory

UNIVERSITY OF CALIFORNIA

Materials & Chemical Sciences Division

RECEIVED
LAWRENCE BERKELEY LABORATORY

MAY 12 1987

Submitted to Acta Crystallographica B

RECEIVED
ACTA CRYSTALLOGRAPHICA B

LEED INTENSITY ANALYSIS OF THE STRUCTURE OF COADSORBED BENZENE AND CO ON Rh(111)

R.F. Lin, G.S. Blackman, M.A. Van Hove,
and G.A. Somorjai

May 1986

TWO-WEEK LOAN COPY

*This is a Library Circulating Copy
which may be borrowed for two weeks.*



LBL-21501
c.2

DISCLAIMER

This document was prepared as an account of work sponsored by the United States Government. While this document is believed to contain correct information, neither the United States Government nor any agency thereof, nor the Regents of the University of California, nor any of their employees, makes any warranty, express or implied, or assumes any legal responsibility for the accuracy, completeness, or usefulness of any information, apparatus, product, or process disclosed, or represents that its use would not infringe privately owned rights. Reference herein to any specific commercial product, process, or service by its trade name, trademark, manufacturer, or otherwise, does not necessarily constitute or imply its endorsement, recommendation, or favoring by the United States Government or any agency thereof, or the Regents of the University of California. The views and opinions of authors expressed herein do not necessarily state or reflect those of the United States Government or any agency thereof or the Regents of the University of California.

LEED INTENSITY ANALYSIS OF THE STRUCTURE
OF COADSORBED BENZENE AND CO ON Rh(111)

submitted to Acta Crystallographica B
September, 1986

R.F. Lin*, G.S. Blackman,
M.A. Van Hove**, and G.A. Somorjai

Materials and Molecular Research Division
Lawrence Berkeley Laboratory and
Department of Chemistry
University of California, Berkeley
Berkeley, California 94720
USA

* Permanent address: Department of Physics, Fudan University, Shanghai,
People's Republic of China.

** Direct inquiries about computational details to this author.

ABSTRACT

A structure of benzene coadsorbed with CO on Rh(111) has been analyzed using low-energy electron diffraction (LEED) interpreted by dynamical calculations. The present structure, Rh(111)-(3x3)-C₆H₆+2CO, complements an earlier result for the system Rh(111)-(3 $\frac{1}{3}$)-C₆H₆+CO, but is distinguished by a different ratio of benzene to CO molecules. The main characteristics of the molecule-metal bonding are substantially confirmed: intact benzene lying flat and centered over hcp-type hollow sites with an expanded C₆ ring, and CO standing upright on the same type of hollow sites. These two structures are also compared and contrasted with a recent analysis of the structure of benzene coadsorbed with CO on Pt(111), for which bridge sites occur and a larger C₆ ring expansion is found.

1. INTRODUCTION

As part of an ongoing study of the structural chemistry of hydrocarbons on transition metal surfaces, we report on two structures of benzene adsorbed on the Rh(111) single-crystal surface in the presence of coadsorbed carbon monoxide. The first structure, Rh(111)- $\begin{pmatrix} 31 \\ 13 \end{pmatrix}$ -C₆H₆+CO, was published before (Van Hove, Lin & Somorjai, 1983 and 1986) and is recalled here for comparison (the $\begin{pmatrix} 31 \\ 13 \end{pmatrix}$ matrix notation is equivalent to the c(2√3x4)rect notation, also used in these References). The second structure, Rh(111)-(3x3)-C₆H₆+2CO, is new and substantially confirms important aspects of the first structure.

Many techniques have been used to study benzene on transition metal surfaces (Nyberg & Richardson, 1979; Tsai & Muetterties, 1982; Massardier, Tardy, Abon & Bertolini, 1983; Surman, Bare, Hofmann & King, 1983; Koel, Crowell, Mate & Somorjai, 1984; Neumann, Mack, Bertel & Netzer, 1985). Our work is based primarily on low-energy electron diffraction (LEED) and high-resolution electron energy loss spectroscopy (HREELS). As was observed by thermal desorption spectroscopy (TDS) and HREELS (Mate & Somorjai, 1985), the (3x3) benzene structure on Rh(111) differs from the $\begin{pmatrix} 31 \\ 13 \end{pmatrix}$ structure in the molecular ratio C₆H₆:CO, namely 1:2 vs. 1:1, respectively.

There also exists a CO-free ordered benzene structure on Rh(111), with a (2√3x3)rect = $\begin{pmatrix} 44 \\ 22 \end{pmatrix}$ superlattice (Mate & Somorjai, 1985). Although this structure has not been analyzed in detail, its principal features are known and provide an interesting comparison with the CO coadsorbate systems. Furthermore, a parallel sequence of benzene/CO structures exists on Pt(111) (Gland & Somorjai, 1973; Mate & Somorjai, 1985), one of which has been structurally

analyzed in detail (Ogletree, Van Hove & Somorjai, 1987). The interaction between the coadsorbates can manifest itself both in ordering and in bonding effects: the long-range order depends on the relative coverage of the two coadsorbed molecules, and each molecule bonds very differently to the metal in the absence of the other molecule.

2. LEED ANALYSIS OF THE (3x3) STRUCTURE

2.1 LEED Experiment

The Rh(111) single-crystal surface was cleaned by repeated cycles of heating in oxygen, argon sputtering, and annealing (Lin, Koestner, Van Hove & Somorjai 1983). Cleanliness was verified by Auger Electron Spectroscopy. The data used for this surface structure analysis were obtained at normal incidence. The crystal was oriented to within $\sim 0.2^\circ$ of normal incidence by slowly varying the θ angle and observing symmetry equivalent beams.

The Rh(111)+(3x3) pattern was obtained by first dosing the crystal with approximately 2/9 monolayer of CO (to provide 2 CO molecules per (3x3) unit cell); then saturating the surface with benzene. This produced a single complete molecular layer on the metal substrate. Calibration of the CO coverage was possible by comparison with the solved Rh(111)-($\sqrt{3}\times\sqrt{3}$)R30°-CO structure, which corresponds to 1/3 monolayer of CO. Carbon monoxide gas of 99.98% purity was used with no further purification. The benzene was dried over a desiccant and degassed using several cycles of freezing with liquid nitrogen followed by pumping with a sorption pump.

LEED intensities were obtained as a function of electron kinetic energy from a standard 4 grid LEED optics by both the photographic method (Lin, Koestner, Van Hove & Somorjai, 1983) and the video-camera method (Ogletree, Katz & Somorjai, 1986) with excellent reproducibility. Because of the possibility of electron beam damage in these organic overlayers, sequential data sets were taken under identical conditions. Subsequent analysis of absolute peak intensities indicated an insignificant amount of beam damage. In our LEED intensity analysis, we have used intensity-energy (I-V) curves for 14 symmetry-inequivalent beams measured at normal incidence, with an energy range of 20-200eV. These beams are labeled (0,-1), (1,-1), (1,-2), (0,-2/3), (2/3,-2/3), (1/3,-2/3), (1/3,-1), (2/3,-1), (2/3,-4/3), (1,-4/3), (0,-4/3), (4/3,-4/3), (4/3,-1/3), (0,-5/3). The LEED pattern and beam labeling are illustrated in Figure 1, together with a real-space representation of the unit cell. The cumulative energy range (added over the 14 beams) was 1144eV.

2.2 LEED Theory

The theory underlying the LEED calculations used to interpret the experimental data has been described elsewhere (Van Hove, Lin & Somorjai, 1986). We give here a summary of the various calculational techniques applied in this work. Our basis is a multiple-scattering theory, called the Combined Space Method and extended to include a number of approximations. The structural search was conducted in steps of increasing theoretical accuracy, as the search narrowed down the list of plausible structures. For the molecular overlayer we started with the kinematic approximation to obtain layer diffraction matrices. Better accuracy was obtained with a near-neighbor

multiple-scattering version of Reverse Scattering Perturbation (RSP), in which multiple scattering paths were allowed to connect only near-neighbor atoms within the overlayer. Also, a full version of RSP was employed, allowing all multiple scattering to full convergence within the overlayer. Finally, the highest accuracy was obtained with Matrix Inversion rather than RSP. In all these cases the substrate and the stacking of the overlayers onto the substrate were treated with full multiple scattering (within the Renormalized Forward Scattering Scheme), before inclusion of coadsorbed CO in addition to benzene. To efficiently compensate for the added computational effort due to coadsorption, we applied Beam Set Neglect (BSN), a powerful approximation to handle large unit cells. Another efficient technique, Kinematic Sublayer Addition (KSLA), was chosen to handle the coadsorbates, for which individual scattering properties (with any amount of internal multiple scattering included) are added kinematically into a set of overlayer diffraction matrices. The exact sequence of calculational techniques used will be shown in the Table of the next section. The final, most accurate calculations are believed to provide a structural accuracy of better than 0.1\AA (this value varies somewhat with the structural parameter), based on a variety of tests carried out during this work and previously.

The nonstructural parameters of the calculations (electron mean-free path, Debye temperature, atomic scattering phase shifts, etc.) were the same as those used in our earlier work (Van Hove, Lin & Somorjai, 1986; and Ogletree, Van Hove and Somorjai, 1986). The number of phase shifts used ($l_{\text{max}} + 1$) was 5 during most of the structural search and 6 in the final stages. Hydrogen was ignored, as usual.

We have applied R-factors to evaluate the level of agreement between theoretical intensities I_t and experimental intensities I_e for the various structural models. We have used the following five R-factors together with their average.

ROS = fraction of energy range with slopes of opposite signs in the experimental and theoretical I-V curves,

$$R1 = 0.75 \int |I_e - cI_t| dE / \int |I_e| dE,$$

$$R2 = 0.5 \int (I_e - cI_t)^2 dE / \int I_e^2 dE,$$

$$RRZJ = 0.5 \int \{ |I_e'' - cI_t''| |I_e' - cI_t'| / (|I_e'| + \max |I_e'|) \} dE / (0.027 \int |I_e| dE),$$

$$RPE = 0.5 \int (Y_e - Y_t)^2 dE / \int (Y_e^2 + Y_t^2) dE, \quad Y(E) = L / (1 + V_{oi}^2 L^2), \quad L = I' / I.$$

Here $c = \int |I_e| dE / \int |I_t| dE$ and the apostrophe denotes differentiation with respect to the energy. RRZJ is the reduced Zanazzi-Jona R-factor, while RPE is Pendry's R-factor, both renormalized with a factor 0.5 to match the scale of the other R-factors (V_{oi} is an estimate of the imaginary part of the inner potential, here 4 eV). We shall mainly use the average over these five R-factors, but we shall also quote 2 x RRZJ and 2 x RPE to allow comparison with other work. These R-factors have been used in many previous surface structure studies with LEED (Van Hove, Lin & Somorjai, 1983; 1986; Ogletree, Van Hove & Somorjai, 1986).

2.3 (3x3) Structures Tested

In many ways, the structural search for the (3x3) structure paralleled that for the $\begin{pmatrix} 3 \\ 1 \\ 3 \end{pmatrix}$ structure (Van Hove, Lin & Somorjai, 1986). Based on

the unit cell size, the TDS data and the HREELS data, as well as the approximate Van der Waals sizes of benzene and CO, the benzene molecules were assumed to lie parallel to the Rh(111) surface, while the CO molecules were taken to stand perpendicularly to the surface. High-symmetry sites were assumed, see Table 1 and Figure 2. Since a free azimuthal rotation of benzene about the surface normal (ϕ -rotation) could not be excluded, that possibility was considered, called "spinning" structure in Table 1. Out-of-plane distortions (bucklings) of the C_6 ring were also considered, with shapes related to that of cyclohexane (C_6H_{12}) in "chair" and "boat" varieties. Because the role of CO was at first not clear, we started with CO-free structures. This left vacancies between the benzene molecules, all or some of which were later filled with individual carbon atoms or ethynylidyne ($C-CH_3$). Table 1 gives the chronological sequence of structures tested.

Then, new TDS and HREELS experiments (Mate & Somorjai, 1985) indicated the presence of about two CO molecules per benzene molecule, the CO molecules being probably in hollow sites. Thus, both vacancies in the benzene layer were filled with CO molecules. The azimuthal orientation of benzene is then most likely constrained by steric hindrance to a value of $\phi=0^\circ$, as exhibited in Figure 2a, b.

In-plane, Kekulé-type distortions were extensively investigated. These consist of alternating long and short C-C bonds within the C_6 rings with C_{3v} symmetry. Two variables can be used to describe a Kekulé distortion (see Figure 2d): a radius r and an angular departure β from 6-fold symmetrical positions. Note that in the benzene adsorption sites preferred

by the LEED analysis (the hollow sites) and with $\phi = 0^\circ$, the Kekulé distortion has the same symmetry as the site itself. Furthermore, no out-of-plane buckling of the C_6 ring respects the site symmetry when $\phi=0^\circ$. Altogether, over 1600 distinct structural geometries were tested.

Representative R-factor contour plots are shown in Figure 3. They illustrate the sensitivity to various structural parameters.

3. Results

Minimizing the R-factors yields our best structure for $Rh(111)-(3 \times 3) - C_6H_6 + 2CO$, illustrated in Figure 4.

In the (3×3) structure, both benzene and CO are centered on hcp-type hollow sites in a compact arrangement, as in the $\begin{pmatrix} 3 & 1 \\ 1 & 3 \end{pmatrix}$ structure. The benzene carbon ring has a spacing of $2.20 \pm 0.05 \text{ \AA}$ to the metal surface with six identical Rh-C bond lengths of $2.30 \pm 0.05 \text{ \AA}$. The corresponding $\begin{pmatrix} 3 & 1 \\ 1 & 3 \end{pmatrix}$ distances are $2.25 \pm 0.05 \text{ \AA}$ and $2.35 \pm 0.05 \text{ \AA}$. A possible Kekulé distortion is found, with $r=1.51 \text{ \AA}$ and $\beta=1.3^\circ$, which yields alternating C-C bond lengths of $1.46 \pm 0.15 \text{ \AA}$ and $1.58 \pm 0.15 \text{ \AA}$ in the (3×3) structure. The corresponding $\begin{pmatrix} 3 & 1 \\ 1 & 3 \end{pmatrix}$ values are $r=1.72 \text{ \AA}$, $\beta=4.5^\circ$ and C-C bond lengths of $1.33 \pm 0.15 \text{ \AA}$ and $1.81 \pm 0.15 \text{ \AA}$. In both cases, the short C-C bonds lie over tops of single metal atoms, while the long C-C bonds form bridges linking pairs of metal atoms.

The optimal metal-carbon spacing for CO in the (3x3) structure is $1.30 \pm 0.10 \text{ \AA}$, giving a Rh-C bond length of $2.02 \pm 0.07 \text{ \AA}$, with a best C-O bond length of $1.1 \pm 0.10 \text{ \AA}$. In the $\begin{pmatrix} 31 \\ 13 \end{pmatrix}$ structure, we had found corresponding values of $1.50 \pm 0.05 \text{ \AA}$, $2.16 \pm 0.04 \text{ \AA}$ and $1.21 \pm 0.05 \text{ \AA}$, respectively. The values of our error bars are based on various considerations: past experience with the uncertainties in the non-structural parameters and with the effects of the data base size, as well as on the R-factor contour plots.

The best (3x3) structure has values of Zanazzi-Jona R-factor, Pendry R-factor and five-R-factor average of 0.24, 0.41 and 0.21, respectively. These can be compared with 0.40, 0.66 and 0.31, respectively, for $\begin{pmatrix} 31 \\ 13 \end{pmatrix}$ and 0.42, 0.54 and 0.28, respectively, for Pt(111)-(2√3x4)rect-2C₆H₆+4CO. In both cases on Rh(111) the muffin-tin zero level is found at $8 \pm 1 \text{ eV}$ below the vacuum zero energy.

4. Discussion

Figure 5 shows our best structure for Rh(111)- $\begin{pmatrix} 31 \\ 13 \end{pmatrix}$ -C₆H₆+CO (Van Hove, Lin & Somorjai, 1986). Figure 6 shows the approximate structure of Rh(111)-(2√3x3)rect-2C₆H₆, in which glide-plane symmetry imposes the choice of bridge site. For this CO-free structure a LEED intensity analysis has not been carried out to investigate the C₆ ring shape and other parameters. For further comparison, the structure found (Ogletree, Van Hove & Somorjai, 1987) for Pt(111)-(2√3x4)rect-2C₆H₆+4CO is shown in Figure 7.

Table 2 compares the present structural result with the two other benzene results on Rh(111) and Pt(111) surfaces, as well as with gas-phase benzene, benzene in organo-metallic complexes, acetylene and ethylene parallel bonded on

Pt(111) and ethynylidyne (CCH_3) bonded on Rh and Pt(111). Also, some theoretical results obtained with the Extended Hückel molecular orbital method are included for benzene on Rh(111). Table 3 makes similar comparisons for the structure of CO on various metal surfaces.

Van Hove, Lin & Somorjai (1986) contains a detailed discussion of a number of points arising out of such comparisons. We shall here summarize those points and focus on new aspects due to the present availability of three distinct benzene surface structures. As discussed in Van Hove, Lin & Somorjai, (1986) the coadsorption of benzene and CO generates new ordering arrangements not present with the separate adsorption of benzene alone or CO alone. The adsorption sites themselves can be modified by coadsorption. The tendency is for benzene to move from bridge sites to hollow sites because of CO coadsorption on Rh(111) (the same hcp-type hollow sites in both structures on Rh(111)). The CO molecules tend towards higher-coordination sites due to coadsorption of benzene, especially on Rh(111). A charge transfer from benzene via the substrate to CO may explain

this behavior. A C-O bond elongation, suggested especially by the Rh(111)- $\begin{pmatrix} 31 \\ 13 \end{pmatrix}$ - $\text{C}_6\text{H}_6+\text{CO}$ structure, is consistent with this picture. Less C-O elongation for Rh(111)- (3×3) - $\text{C}_6\text{H}_6+2\text{CO}$ and Pt(111)- $(2\sqrt{3} \times 4)$ rect- $2\text{C}_6\text{H}_6+4\text{CO}$ might be explained by the sharing of benzene-donated charge among more CO molecules (this is also consistent with a slight increase of the C-O stretch frequency which occurs at the same time). It is not clear at this point why the Rh-C bond length for CO appears to differ considerably between the $\begin{pmatrix} 31 \\ 13 \end{pmatrix}$ and the (3×3) structures: $2.16 \pm 0.04 \text{ \AA}$ and $2.02 \pm 0.07 \text{ \AA}$, respectively.

The benzene adsorption site varies as is shown in Table 2. It may be added that, in the absence of CO, benzene is probably located in bridge sites both on

Rh(111) (Van Hove, Lin & Somorjai, 1986) and on Pt(111) (Lin, Koestner, Van Hove & Somorjai, 1983). Our results indicate that the C_6 ring can distort in a way compatible with the site symmetry, i.e. with $C_{3v}(\sigma_d)$ symmetry over hollow sites and C_{2v} symmetry over bridge sites (or C_s symmetry if deeper metal layers are taken into account). The main effect of adsorption is a C_6 ring expansion, such that the mean ring radius is $1.58 \pm 0.15 \text{ \AA}$, $1.51 \pm 0.15 \text{ \AA}$ and $1.72 \pm 0.15 \text{ \AA}$, respectively for Rh(111) + $\begin{pmatrix} 31 \\ 13 \end{pmatrix} - C_6H_6 + CO$, Rh(111) + (3x3) - $C_6H_6 + 2CO$ and Pt(111) + (2√3x4)rect - $2C_6H_6 + 4CO$. In the $\begin{pmatrix} 31 \\ 13 \end{pmatrix}$ structure we find also a strong variation between C-C bonds (three short bonds and three long bonds), which is not as clearly apparent in the two other structures (we must keep in mind the relatively large error bars of $\pm 0.15 \text{ \AA}$ on these distances). As mentioned in more detail in Van Hove, Lin, & Somorjai, (1986) similar but weaker distortions are found in organometallic complexes. New results (Gomez-Sal, Johnson, Lewis, Raithby & Wright, 1985) are now available for two complexes containing benzene symmetrically placed against a metal triangle, $Ru_6C(CO)_{11}(C_6H_6)_2$ and $Os_3(CO)_9(C_6H_6)$. As Table 2 shows, these exhibit the Kekulé-type distortion of our $\begin{pmatrix} 31 \\ 13 \end{pmatrix}$ structure. Although it is less strong, this distortion also features a C_6 ring expansion to a radius of $1.44 \pm 0.02 \text{ \AA}$. Similar expansions are found with Near Edge X-ray Absorption Fine Structure (NEXAFS) measurements for acetylene and ethylene parallel-bonded to the Pt(111) surface (Stöhr, Sette & Johnson, 1984). The extended-Hückel results (Garfunkel, Minot, Gavezzotti & Simonetta 1986) also predict a ring expansion, to about 1.52 \AA , and a possible Kekulé-type distortion with C-C bond lengths of up to 1.50 and 1.64 \AA , for the short and long bonds. Ethynylidyne (CCH_3) species

have C-C bonds perpendicular to the surface. Although these bonds are not in direct contact with the metal, unlike the case of benzene, they provide a valuable reference point for comparison of C-C bond lengths: see Table 2.

Recent measurements with angle-resolved ultraviolet photoelectron spectroscopy have been made for benzene with and without CO on Rh(111) (Neumann, Mack, Bertel & Netzer, 1985). The case with CO had the (3x3) pattern, while the CO-free case is claimed to have the $\begin{pmatrix} 3 \\ 1 \\ 3 \end{pmatrix}$ pattern (our results would suggest that this pattern is due to some coadsorbed CO. These data appear to indicate that no deviation from six-fold symmetry occurs, i.e. that all C-C bonds in the C₆ ring are equally long. Our results may well be consistent with these conclusions. In the (3x3) case, our Kekulé-type distortion is possibly slight, while in the CO-free case, our analogous result on Pt(111) also shows small variations between C-C bond lengths for bridge-site adsorption. It is also possible that photoemission is insensitive to small deviations from 6-fold symmetry.

Finally, a connection can be suggested between our results and the catalytic reactivity of Rh and Pt for benzene reactions. The platinum (111) crystal face is an excellent catalyst for the production of benzene from n-hexane or n-heptane (dehydrocyclization). This is an important reaction that is utilized in petroleum refining to produce high octane gasoline. The Rh(111) crystal face however, cannot carry out this catalytic reaction because of the rapid fragmentation of benzene on the metal surface (hydrogenolysis) under the reaction conditions. It would be tempting to correlate the surface structures that adsorbed benzene forms on these two transition metal surfaces

to their catalytic behavior. Perhaps the large Kekulé distortion of the adsorbed aromatic molecule observed in one of our structures on rhodium is indicative of preferential C-C bond breaking to produce CH and C₂H fragments, which occurs as the temperature is increased (Koel, Crowell, Bent, Mate & Somorjai, 1986). Benzene chemisorbed on the Pt(111) crystal face is less systematically distorted, exhibiting only a more uniform expansion of the ring. Perhaps such a structure is indicative of a benzene intermediate on the metal surface that can desorb intact at the higher temperatures and pressures of the catalytic reaction. Future studies will test further the possible correlation between molecular surface structures and catalytic reaction intermediates.

ACKNOWLEDGEMENTS

We thank C. Minot, M. Simonetta, A. Gavezzotti and E. Garfunkel for fruitful discussions, made possible by a NATO US-France exchange grant and an NSF US-Italy exchange grant. This work was supported by the Director, Office of Energy Research, Office of Basic Energy Sciences, Materials Science Division, of the U. S. Department of Energy under Contract Number DE-AC03-76SF00098. Super-computer time was also provided by the Office of Energy Research of the Department of Energy.

REFERENCES

- Andersson, S. and Pendry, J. B. (1979), Phys. Rev. Letters 43, 363.
- Behm, R. J., Christmann, K., Ertl, G. and Van Hove, M. A. (1980), J. Chem. Phys. 73, 2984.
- Chini, P., Longoni, G. and Albano, V.G. (1976), Adv. Organomet. Chem. 14, 285.
- Garfunkel, E.L., Minot, C., Gavezotti, A. and Simonetta, M. (1986), Surf. Sci. 167, 177.
- Gland, J.L. and Somorjai, G.A. (1973), Surf. Sci. 38, 157.
- Gomez-Sal, M.P., Johnson, B.F.G., Lewis, T., Raithby, P.R. and Wright, A.H. (1985), J. Chem. Soc., Chem. Commun., 1682.
- Horsley, J.A., Stöhr, J., Hitchcock, A.P., Newbury, D.C., Johnson, A.L. & Sette F. (1985), J. Chem. Phys. 83, 6099.
- Horsley, J.A., Stöhr, J. & Koestner, R.J. (1985), J Chem. Phys. 83, 3146.
- Kesmodel, L.L., Dubois, L.H. and Somorjai, G.A. (1979), J. Chem. Phys. 70, 2180.
- Koel, B.E., Crowell, J.E., Bent, B.E., Mate, C.M. and Somorjai, G.A. (1986), J. Phys. Chem. 90, 2949.
- Koel, B.E., Crowell, J.E., Mate, C.M. and Somorjai, G.A. (1984), J. Phys. Chem. 88, 1988.
- Koestner, R.J., Van Hove, M.A., Frost, J.C. and Somorjai, G.A. (1981), Surf. Sci. 107, 439.
- Koestner, R.J., Van Hove, M.A. and Somorjai, G.A. (1982), Surf Sci 121, 321.
- Lin, R.F., Koestner, R.J., Van Hove, M.A. and Somorjai, G.A. (1983), Surf. Sci. 134, 161.

References cont'd

- Massardier, J., Tardy, B., Abon, M. and Bertolini, J.C. (1983), Surf. Sci. 126, 154.
- Mate, C.M. and Somorjai, G.A. (1985), Surf. Sci. 160, 542.
- Michalk, G., Moritz, W., Pfnür, H. and Menzel, D. (1983), Surf. Sci. 129, 92.
- Neumann, M., Mack, J.U., Bertel, E. and Netzer, F.P. (1985), Surf. Sci. 155, 629.
- Nyberg, G.L. and Richardson, N.V. (1979), Surf. Sci. 85, 335.
- Ogletree, D.F., Katz, J.E. and Somorjai, G.A. (1986), Rev. Sci. Instrum. 57, 3012.
- Ogletree, D.F., Van Hove, M.A. and Somorjai, G.A. (1986), Surf. Sci. 173, 351.
- Ogletree, D.F., Van Hove, M.A. and Somorjai, G.A. (1987), in preparation.
- Stöhr, J., Sette, F. and Johnson, A.L. (1984), Phys. Rev. Letters 53, 1684.
- Surman, M., Bare, S.R., Hofmann, P. and King, D.A. (1983), Surf. Sci. 126, 349.
- Tong, S.Y., Maldonado, A., Li, C.H. and Van Hove, M.A. (1980), Surf. Sci. 94, 73.
- Tsai, M.C. and Muetterties, E.L. (1982), J. Phys. Chem. 86 5067.
- Van Hove, M.A., Lin, R.F. and Somorjai, G.A. (1983), Phys. Rev. Letters 51, 778.
- Van Hove, M.A., Lin, R.F. and Somorjai, G.A. (1986), J. Amer. Chem. Soc; 108, 2532.
- Wang, P.K., Slichter, C.P. and Sinfelt, J.H. (1985), J. Phys. Chem. 89, 3606.

TABLE 1: Structures tested by LEED intensity calculations

Compo- sition	Site ^a	$\phi(^{\circ})^b$	$d_{\perp M-C_6}(\text{\AA})^c$	Buckling ^d	$d_{C-C}(\text{\AA})^e$	Method ^f
C_6H_6	aABC, bABC, cABC	0, 15, 30	1.2(.3)3.9	none	1.397	kinematic
"	aABC	0, 30	1.5(.1)1.9	"	"	partial & full RSP
"	bABC	"	2.9(.1)3.3	"	"	"
"	cABC	"	1.9(.1)2.3	"	"	"
"	aABC	spinning ^g	1.5(.1)1.9	"	"	kinematic
"	bABC	"	2.9(.1)3.3	"	"	"
"	cABC	"	1.9(.1)2.3	"	"	"
"	dABC	0, 30 spinning ^g	1.2(.2)4.0	"	"	"
"	aABC, bABC, cABC	0	1.2(.3)3.9	"	1.54	"
"	aABC, bABC, cABC	0	1.2(.3)3.9	"	(1.33, 1.54) ^h	"
"	dABC	0, 30	1.2(.2)4.0	"	1.54	"
"	dABC	0	"	"	(1.33, 1.54) ^h	"
"	"	"	"	"	(1.54, 1.33) ^h	"
"	aABC, bABC, cABC	± 30	1.2(.3)3.9	chair ⁱ	1.54	"
"	dABC	0	1.2(.2)4.0	boat up ^j .3\AA, .5\AA	"	"
"	"	"	"	boat down ^j .3\AA, .5\AA	"	"
"	aABC, bABC, cABC	0.30	1.6(.1)2.5	none	(1.33, 1.64 (.43)3.36) ^h	"
"	bABC, cABC	0	1.65(.15) 2.25	"	1.397	"

TABLE I: Structures tested by LEED intensity calculations (Cont'd.)

Composition	Site ^a		$\phi(^{\circ})^b$	$d_{\perp C-C_6}(\text{\AA})^l$	$d_{C-C}(\text{\AA})^e$	$d_{\perp M-C_1}(\text{\AA})^k$	Method ^f
	C_6H_6	C					
C_6H_6+C	bABC	bABC ^m	0	.55(.15)1.15	1.397	1.10(.15)1.70	BSN+partial RSP
"	cABC	cABC ^m	"	"	"	"	"
"	bABC	bABC ^m	"	.40(.2)1.60	"	1.10(.20)1.50	BSN+full RSP
"	cABC	cABC ^m	"	"	"	"	"
$C_6H_6+2C^n$	bABC	2xbABC	"	.55(.15)1.15	"	1.10(.15)1.70	BSN+partial RSP
"	cABC	2xcABC	"	"	"	"	"
$C_6H_6+2C^o$	bABC	bABC ^m	"	"	"	"	"
"	cABC	cABC ^m	"	"	"	"	"

Composition	Site ^a		$\phi(^{\circ})^b$	$d_{\perp C-C_6}(\text{\AA})^s$	Ring Distortion ^p		$d_{\perp M-CO}(\text{\AA})^r$	$d_{C-O}(\text{\AA})^q$	Method ^f
	C_6H_6	CO			r(\text{\AA})	$\beta(^{\circ})$			
C_6H_6+2CO	aABC	2xaABC	0	-.2(-.2)-.8	1.397	0	1.3(.1)2.4	1.15	BSN+KSLA+RSP
"	bABC	2xbABC	"	.55(.2)1.15	"	"	"	"	"
"	cABC	2xcABC	"	"	"	"	"	"	"
"	dABC	2xdABC	0,30	.25(.2).85	"	"	1.3(.1)1.8	"	"
"	bABC	2xbABC	0	.5(.2)1.1	1.2(.17) 1.71	-5.0(2.5) 7.5	1.25(.05)1.50	"	BSN+KSLA+MINV (6 phase shifts)
"	"	"	"	"	1.397	0	"	"	"
"	dABC	2xdABC	"	"	"	"	1.3(.1)1.8	"	"
"	bABC	2xbABC	"	.9	1.2(.17) 1.71	$\pm 3.75, 7.5$	1.15(.05)1.4	"	"
"	"	"	"	.5(.2)1.1	1.51	-1.3	"	1.15(.05)1.25	"

NOTES TO TABLE 1

- a. aABC = adsorbate centered on top site, bABC = on hcp-hollow site, cABC = on fcc-hollow site, dABC = on bridge site.
- b. Azimuthal orientation of C_6 ring (see Figure 2a, b).
- c. Smallest layer spacing between metal atom nuclei and C_6 nuclei; notation $d_1(\Delta d)d_2$ implies values from d_1 to d_2 in steps of Δd .
- d. Out-of-plane distortion of C_6 ring, if any.
- e. C-C bond length(s) in C_6 ring.
- f. Computational method (5 phase shifts used, unless otherwise noted);
kinematic = all kinematic in overlayer; "partial RSP" refers to near-neighbor multiple scattering only; RSP = Reverse Scattering Perturbation;
BSN = Beam Set Neglect; KSLA = Kinematic Sublayer Addition; M INV = Matrix Inversion instead of RSP.
- g. "Spinning" $-C_6H_6$ molecules are achieved by averaging among overlayers with different values of ϕ between 0° and 60° .
- h. Kekulé distortion with alternating short and long C-C bonds.
- i. Cyclohexane C_6 structure in chair arrangement, using tetrahedral C-C-C angles.

Notes to Table 1 cont'd

- j. Cyclohexane C_6 structure in boat arrangement, with tips tilted up or down with respect to C_6 median plane ($//$ surface plane) by 0.3 or 0.5Å.
- k. Smallest layer spacing between metal atom nuclei and carbon nuclei of coadsorbate.
- l. Smallest layer spacing between single-carbon nuclei and C_6 nuclei.
- m. Two bABC and two cABC sites are available for C, inequivalent with respect to the C_6H_6 orientation: both were tried.
- n. Two individual C atoms per unit cell.
- o. One pair of carbon atoms, one above the other a distance $d_{\perp CC} = 1.15\text{Å}$ and 1.45Å, similar to ethynidyne.
- p. Kekulé distortions only, characterized by r and β (see Figure 2d).
- q. C-O bond length (C-O bond always perpendicular to surface).
- r. Smallest layer spacing between metal atom nuclei and C nuclei of CO.
- s. Smallest layer spacing between C nuclei of CO and C_6 nuclei.

TABLE 2. ADSORPTION GEOMETRIES OF BENZENE

SYSTEM	$d_{C-C}^{<} (\text{Å})$	$d_{C-C}^{>} (\text{Å})$	$d_{LM-C} (\text{Å})$	$d_{M-C} (\text{Å})$	Site
Rh(111)-c(2√3x4)rect-C ₆ H ₆ +CO ^a	1.33±0.15	1.81±0.15	2.25±0.05	2.35±0.05	hollow
Rh(111)-(3x3)-C ₆ H ₆ +2CO ^b	1.46±0.15	1.58±0.15	2.20±0.05	2.30±0.05	hollow
Rh(111)-(3x3)-C ₆ H ₆ (theory) ^c	1.50	1.64	2.1	2.15	hollow
Pt(111)-(2√3x4)rect-2C ₆ H ₆ +4CO ^d	1.65±0.15	1.76±0.15	2.10±0.10	2.25±0.10	bridge
Pt(111)-C ₆ H ₆ disordered ^e	1.40±0.02				
C ₆ H ₆ on metal clusters ^f	1.39	1.48		2.27-2.32	hollow
C ₆ H ₆ molecule	1.397				
Pt(111)-(2x2)-C ₂ H ₃ (ethylidyne) ^g	1.50±0.1		1.20±0.1	2.00±0.07	hollow
Rh(111)-(2x2)-C ₂ H ₃ (ethylidyne) ^h	1.45±0.10		1.31±0.1	2.03±0.07	hollow
Pt(111)-C ₂ H ₃ (ethylidyne) ⁱ	1.49±0.02				
Pt(111)-C ₂ H ₃ (ethylidyne) ^j	1.47±0.03				
C ₂ H ₆ molecule	1.54				
Pt(111)-C ₂ H ₄ ^k	1.49±0.03				
C ₂ H ₄ molecule	1.33				
Pt(111)-C ₂ H ₂ ^k	1.45±0.03				
C ₂ H ₂ molecule	1.20				

a. Van Hove, M.A., Lin, R.F. & Somorjai, G.A. (1986); b. This work; c. Garfunkel, E.L., Minot, C., Gavezzotti, A. & Simonetta, M. (1986); d. Ogletree, D.F., Van Hove, M.A. & Somorjai, G.A. (1987); e. Horsley, J.A., Stöhr, J., Hitchcock, A.P., Newbury, D.C., Johnson, A.L. & Sette, F. (1985); f. Gomez-Sal, M.P., Johnson, B.F.G., Lewis, T., Raithby, P.R. & Wright, A.H. (1985); g. Kesmodel, L.L., Dubois, L.H. & Somorjai, G.A. (1979); h. Koestner, R.J., Van Hove, M.A. & Somorjai, G.A. (1982); i. Wang, P.K., Slichter, C.P. & Sinfelt, J.H. (1985); j. Horsley, J.A., Stöhr, J. & Koestner, R.J. (1985); k. Stöhr, J., Sette, F. & Johnson, A.L. (1984).

TABLE 3. ADSORPTION GEOMETRIES OF CARBON MONOXIDE

SYSTEM	$d_{\perp M-C}(A)$	$d_{M-C}(A)$	$d_{C-O}(A)$	Site
Pt(111)-c(4x2)-2CO ^a	1.85±0.1	1.85±0.1	1.15±0.05	top
Rh(111)-($\sqrt{3}\times\sqrt{3}$)R30°-CO ^b	1.55±0.1	2.08±0.07	1.15±0.05	bridge
Rh(111)-(2x2)-3CO ^c	1.95±0.1	1.95±0.1	1.07±0.1	top
	1.52±0.1	1.94±0.1	1.15±0.1	top
	2.03±0.1	2.03±0.07	1.15±0.1	bridge
Ni(100)-c(2x2)-CO ^{d,e}	1.75±0.1	1.75±0.1	1.15±0.1	top
Cu(100)-c(2x2)-CO ^e	1.90±0.1	1.90±0.1	1.13±0.1	top
Pd(100)-(2 $\sqrt{2}\times\sqrt{2}$)R45°-2CO ^f	1.36±0.1	1.93±0.07	1.15±0.1	bridge
Ru(0001)-($\sqrt{3}\times\sqrt{3}$)R30°-CO ^g	2.00±0.07	2.00±0.07	1.10±0.1	top
Rh(111)-c(2 $\sqrt{3}\times 4$)rect-CO+C ₆ H ₆ ^h	1.50±0.05	2.16±0.04	1.21±0.05	hollow
Rh(111)-(3x3)-2CO+C ₆ H ₆ ⁱ	1.30±0.1	2.02±0.07	1.17±0.1	hollow
Pt(111)-(2 $\sqrt{3}\times 4$)rect-4CO+2C ₆ H ₆ ^j	1.45±0.1	1.99±0.07	1.15±0.1	bridge
CO on metal clusters ^k		2.17-2.23	1.15-1.22	hollow
CO on metal clusters ^k		2.00-2.09	1.07-1.18	bridge
CO on metal clusters ^k		1.82-1.91	1.01-1.18	top

a. Ogletree, D.F., Van Hove, M.A., & Somorjai (1986); b. Koestner, R.J., Van Hove, M.A., Frost, J.C. & Somorjai, G.A. (1981); c. Koestner, R.J., Van Hove, M.A., & Somorjai, G.A. (1982); d. Tong, S.Y., Maldonado, A., Li, C.H., & Van Hove, M.A. (1980); e. Andersson, S. & Pendry, J.B. (1979); f. Behm, R.J., Christmann, K., Ertl, G. & Van Hove, M.A. (1980); g. Michalk, G., Moritz, W., Pfnür, H. & Menzel, D. (1983); h. Van Hove, M.A., Lin, R.F. & Somorjai, G.A. (1986); i. This work; j. Ogletree, D.F., Van Hove, M.A. & Somorjai, G.A. (1986); k. Chini, P., Longoni, G., Albano, V.G. (1976)

FIGURE CAPTIONS

- Figure 1. Schematic LEED pattern with beam labeling (panel a) and corresponding surface unit cell for (3x3) overlayer on Rh(111) (panel b).
- Figure 2. Panels a and b show the molecular packing within the (3x3) overlayer on Rh(111) with the help of Van der Waals contours, for two benzene orientations ($\phi=0^\circ$ and 30°) and two CO molecules per unit cell. Panel c represents four "registries" of the (3x3) overlayer (with $\phi=0^\circ$) with respect to the substrate. The benzenes are represented by rings of carbons and hydrogens, the CO by crosses. Note atoms in the second metal layer, represented by dots and distinguishing registries bABC and cABC. The Kekulé distortion of benzene is defined in panel d.
- Figure 3. R-factors contour plots for pairs of structural variables; related are the CO and C_6H_6 heights over the metal surface ($d_{\perp Rh-C_1}$, and $d_{\perp C_1-C_6}$, respectively), benzene Kekulé distortions (given by r and β , see Figure 2d) and the C-O bond length.
- Figure 4. Optimal structure for Rh(111)-(3x3)- C_6H_6+2CO , in side view at top and plan view at bottom. Van der Waals shapes are used. The CO molecules are shown shaded. The hydrogen positions are guessed.

Figure Captions cond't

Figure 5. As Figure 4 for Rh(111)-c(2√3x4)rect-C₆H₆+CO, from Van Hove, M.A., Lin, R.F. and Somorjai, G.A. (1986).

Figure 6. As Figures 4 and 5 for Rh(111)-(2√3x3)rect-2C₆H₆, from Mate, C.M. and Somorjai, G.A. (1985). Dashed lines indicate glide planes perpendicular to the surface, the short dashed ones not applying to the deeper metal layers.

Figure 7. As Figures 4 and 6 for Pt(111)-(2√3x4)rect-2C₆H₆+4CO, from Ogletree, D.F., Van Hove, M.A. and Somorjai, G.A. (1987).

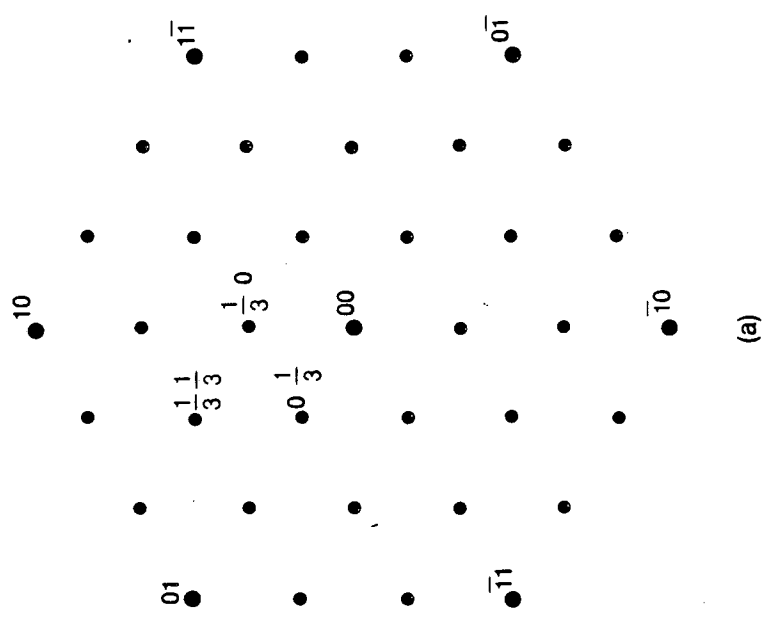
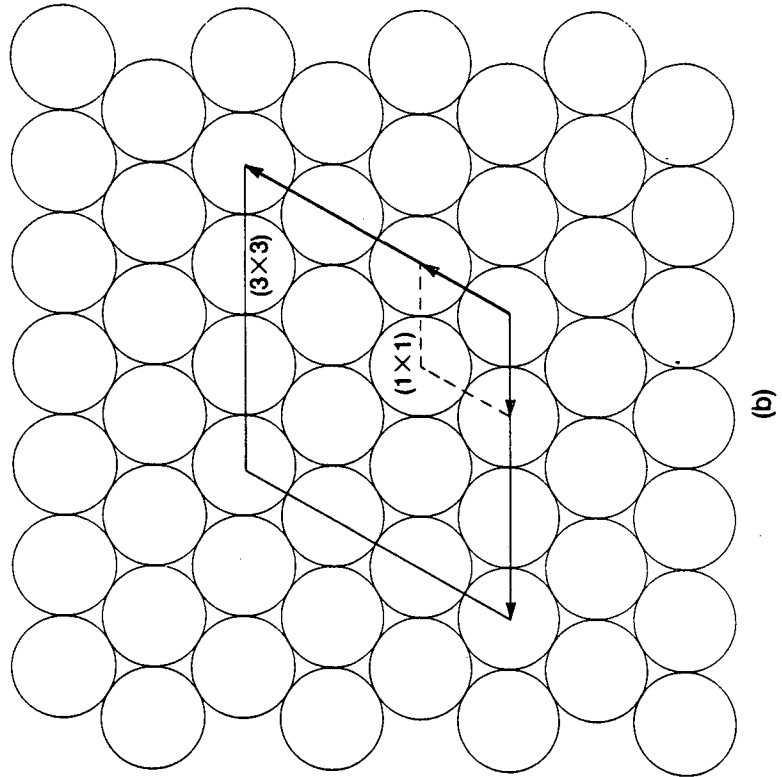
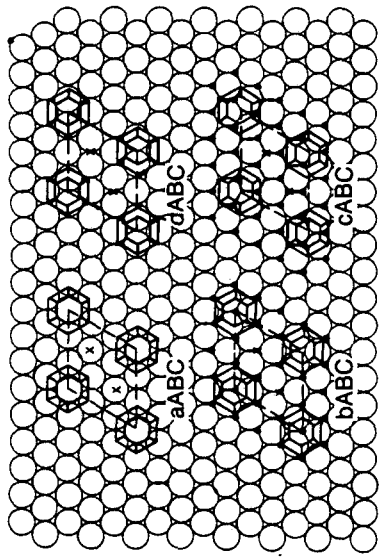
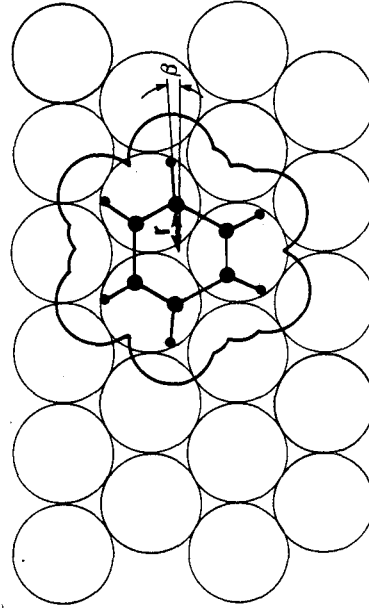


Figure 1

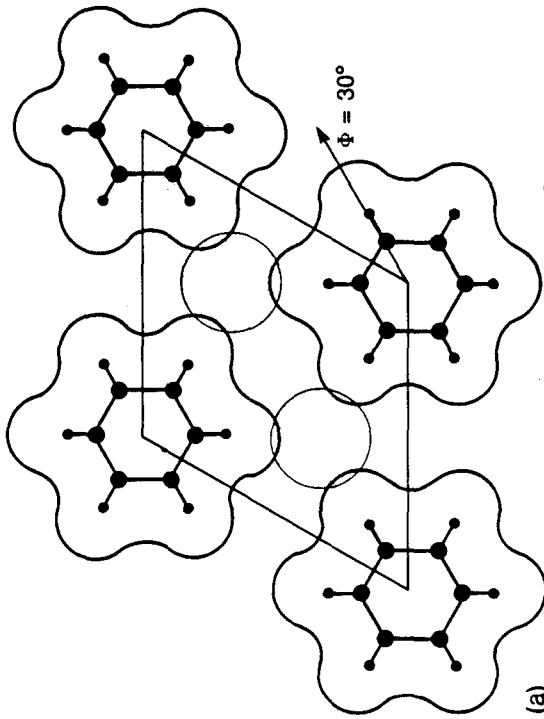
XBL 863-10697



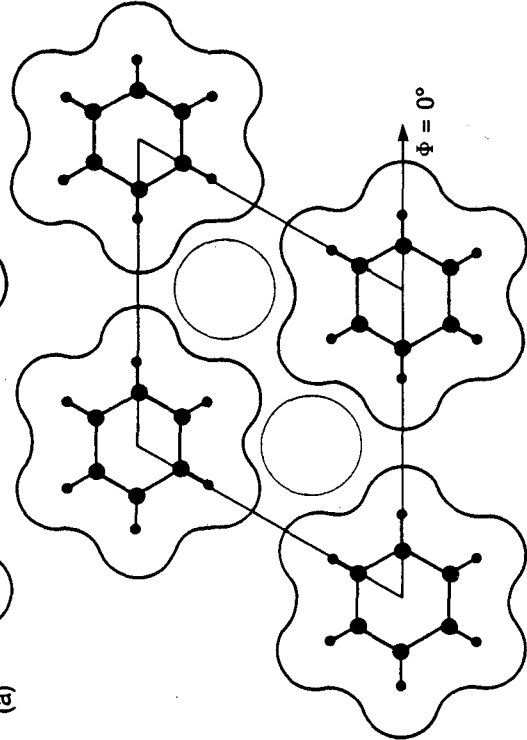
(c)



(d)



(a)

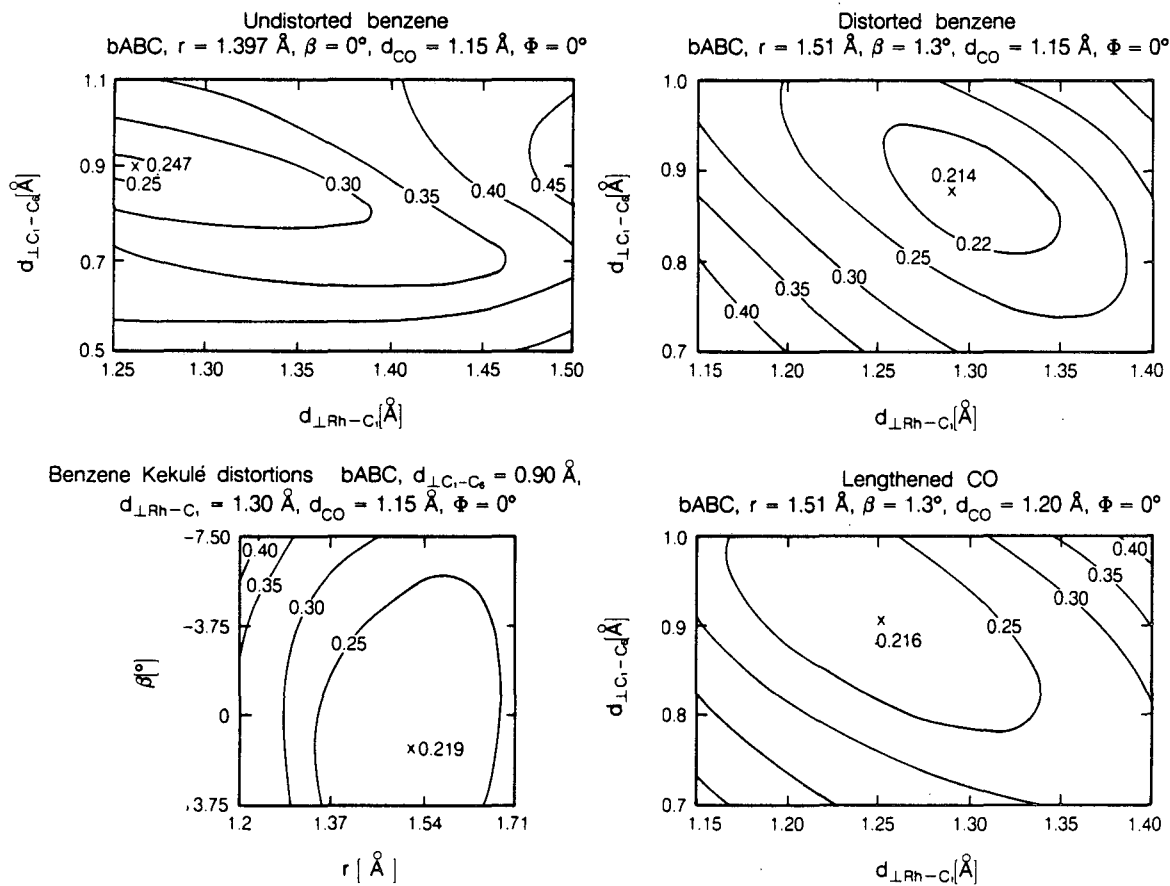


(b)

XBL 863-10703

Figure 2

Rh(111) - (3x3) - C₆H₆ + 2CO
R-factor contour plots



XBL 863-10704

Figure 3

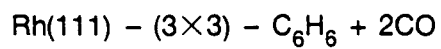
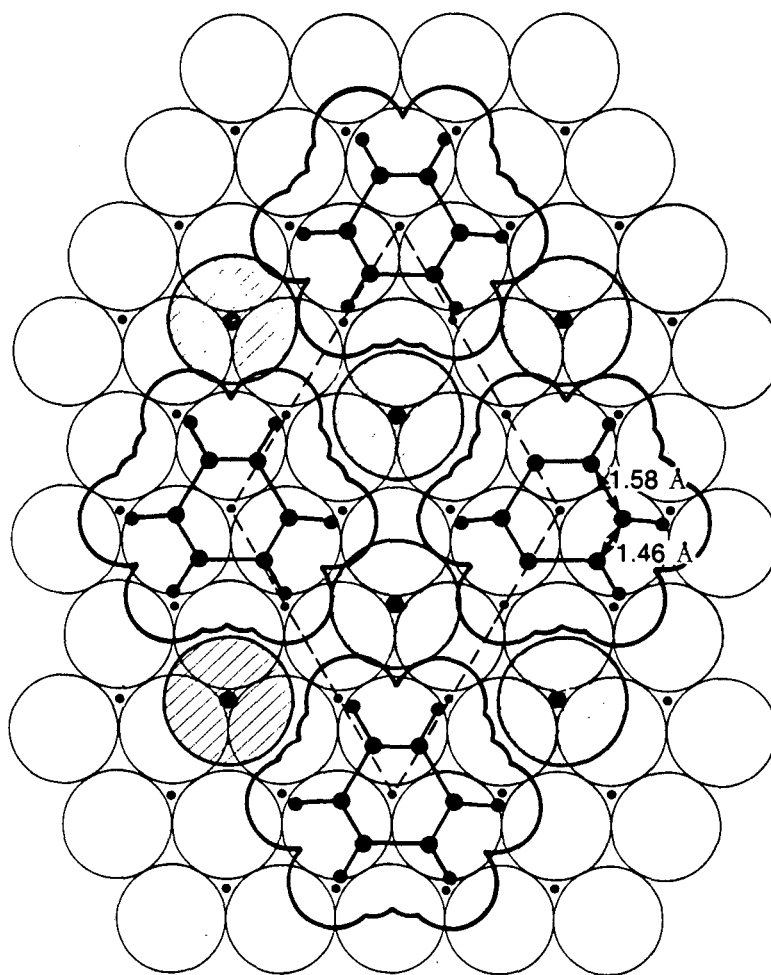
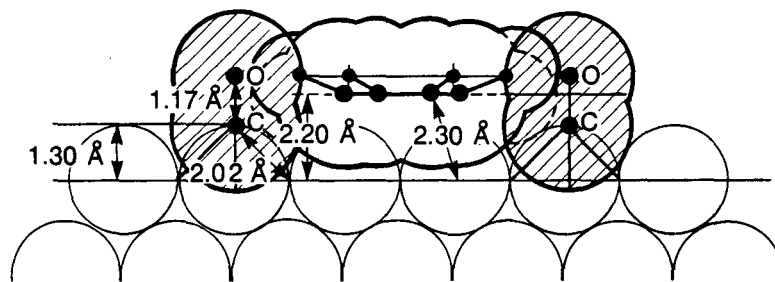
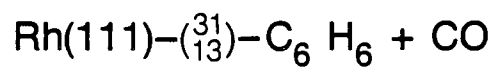
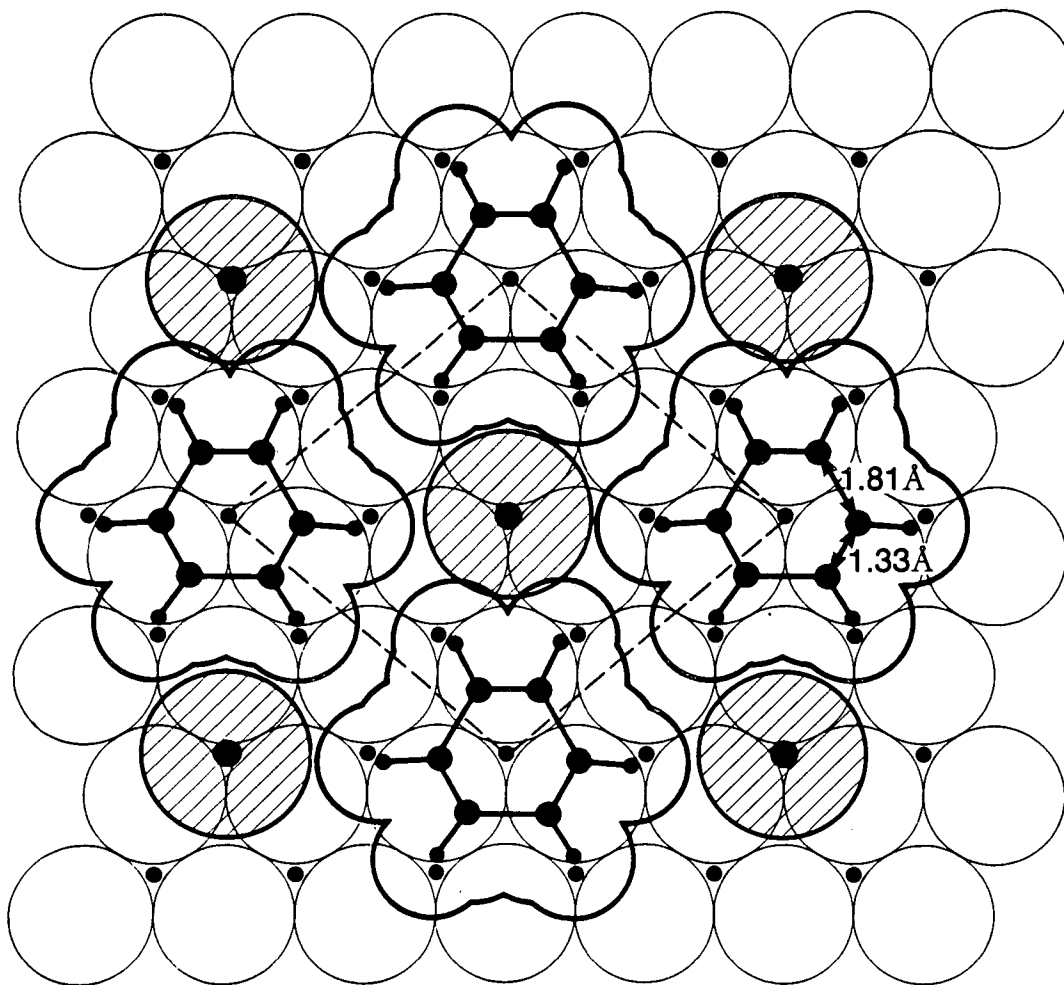
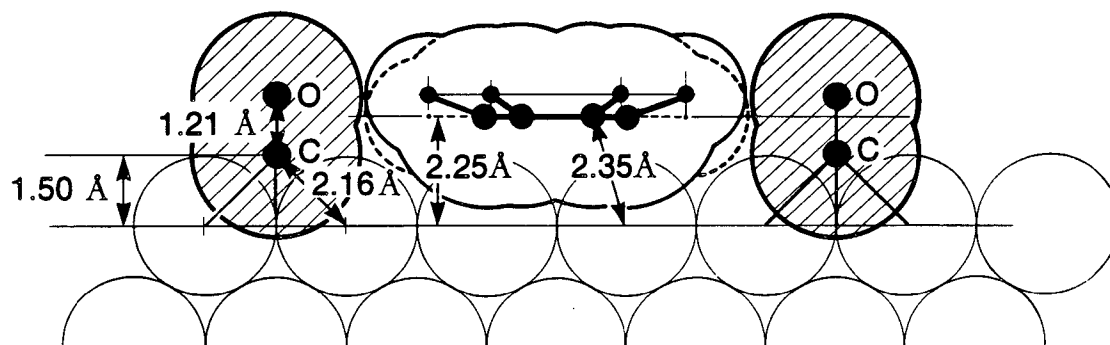


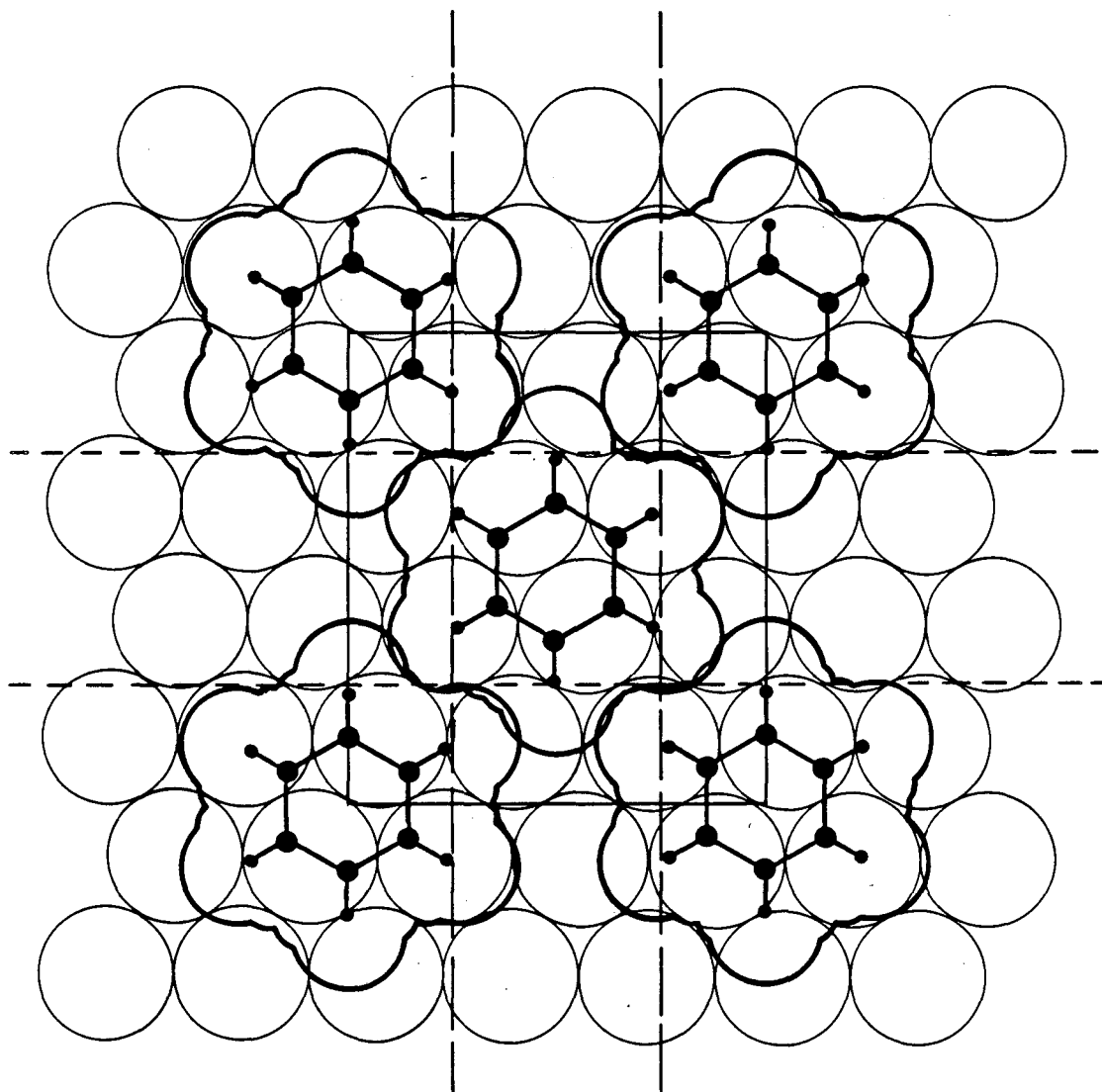
Figure 4

XBL 863-10701



XBL 851-9917 A

Figure 5



$\text{Rh}(111) - (2\sqrt{3} \times 3)\text{rect} - 2\text{C}_6\text{H}_6$

Figure 6

XBL 863-10699

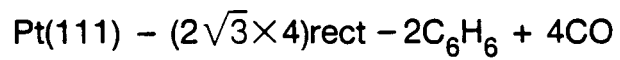
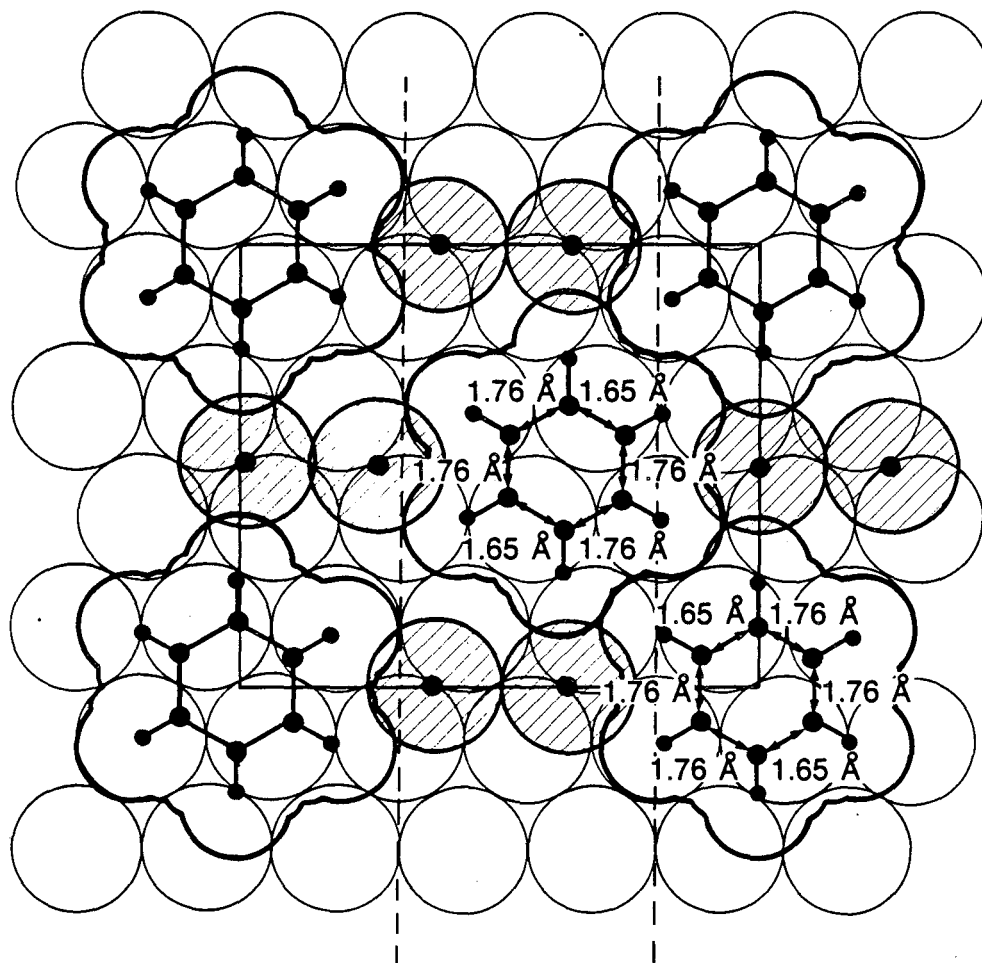
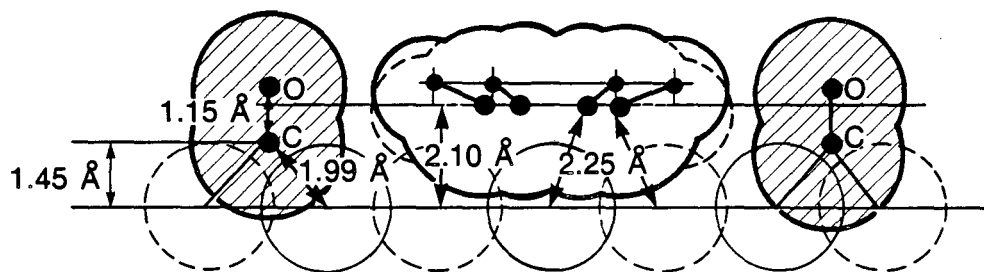


Figure 7

XBL 867-2543

This report was done with support from the Department of Energy. Any conclusions or opinions expressed in this report represent solely those of the author(s) and not necessarily those of The Regents of the University of California, the Lawrence Berkeley Laboratory or the Department of Energy.

Reference to a company or product name does not imply approval or recommendation of the product by the University of California or the U.S. Department of Energy to the exclusion of others that may be suitable.

*LAWRENCE BERKELEY LABORATORY
TECHNICAL INFORMATION DEPARTMENT
UNIVERSITY OF CALIFORNIA
BERKELEY, CALIFORNIA 94720*